# Water molecular state in 1-hexylpyridinium hexafluorophosphate: Water mean cluster size as a function of water concentration

Abdellatif Dahi, Kateryna Fatyeyeva, Corinne Chappey, Dominique Langevin, Stéphane Marais

# Water molecular state in 1-hexylpyridinium hexafluorophosphate: water mean cluster size as a function of water concentration

Abdellatif Dahi, Kateryna Fatyeyeva*, Corinne Chappey, Dominique Langevin, Stéphane Marais

Normandie Univ., UNIROUEN, INSA ROUEN, CNRS, PBS, 76000 Rouen, France

*Corresponding author: kateryna.fatyeyeva@univ-rouen.fr

## Abstract

The water sorption behavior of representative pyridinium-based ionic liquid (IL), 1-hexylpyridinium hexafluorophosphate ([$C_6$Py][$PF_6$]), was studied over the whole range of the water activity *a* using a continuous gravimetric method. The analysis of the water sorption isotherm using the combination of a two-mode sorption (i.e. Henry-clustering) allowed to better understand [$C_6$Py][$PF_6$]-water interactions. At low and intermediate activity ($a \leq 0.8$), the water molecules revealed a very low affinity to [$C_6$Py][$PF_6$] and, consequently, the water uptake was rather low. On the contrary, at high water activity ($a > 0.8$), the water uptake increased exponentially and the water clustering easily occurred. The constant of the Henry-clustering equation as well as the water clustering mechanism in [$C_6$Py][$PF_6$] were discussed and compared to those of imidazolium-based ILs: 1-hexyl-3-methylimidazolium hexafluorophosphate [$C_6C_1$im][$PF_6$] (water-immiscible IL) and 1-butyl-3-methylimidazolium tetrafluoroborate [$C_4C_1$im][$BF_4$] (water-miscible IL). It is shown that the sorption of water molecules by pyridinium-based ILs is controlled not only by the anion's nature, but also by the cation's nature. Moreover, the Zimm-Lundberg theory was used to determine the water mean cluster size (MCS) in [$C_6$Py][$PF_6$], [$C_6C_1$im][$PF_6$] and [$C_4C_1$im][$BF_4$]. The MCS results confirmed the strong capacity of water molecules to be aggregated in [$C_6$Py][$PF_6$]. In order to have a deeper insight into the water molecular state, infrared spectroscopy measurements were carried out as a function of the relative humidity value and the obtained results were correlated with the results of water sorption isotherms. It is found that at high water activity ($a > 0.8$), sorbed water molecules are strongly linked with ILs by hydrogen bonds and, therefore, are easily aggregated.

**Keywords**: room temperature ionic liquids, pyridinium-based cations, water sorption, mean cluster size, water molecular state.

## Introduction

Room-temperature ionic liquids (RTILs) are becoming an interesting class of solvents for different applications. They possess attractive chemical and physical properties, and present several advantages compared to conventional solvents, such as good chemical and thermal stability, low volatility, non-flammability, and excellent and adjustable solvent properties[1-4].

The most intensively studied class of RTILs is imidazolium-based RTILs. Nevertheless, pyridinium-based RTILs progressively attract attention recently. De los Rios *et al.* studied the use of alkylpyridinium-based cations combined with various anions as reaction media for the direct transesterification of sunflower-seed oil with methanol[5]. Padró *et al.* studied the partition coefficients of several compounds, some of them of biological and pharmacological interest, between water and RTILs based on the imidazolium, pyridinium, and phosphonium cations[6]. Zhang *et al.* showed that uranium formed various complexes with imidazolium- and pyridinium-based RTILs[7]. They came to conclusion that these RTILs might not only be useful in the extraction of uranium, but also showed high potential in the bioremediation of uranium waste stream. Behar *et al.* showed that the pulse radiolysis in alkylpyridinium-based RTILs allowed the production of a variety of radicals and the measurement of absolute rate constants of the reduction and oxidation of different molecules[8]. Siyuthin *et al.* showed that RTILs containing pyridinium cations and [$PF_6$] anion efficiently catalyzed the asymmetric aldol reaction between aldehydes and ketones in the presence of water to generate aldols with high distereo- and enantio-selectivity[9]. Abdolmohammad-Zadeh *et al.* used 1-hexylpyridinium hexafluorophosphate ([$C_6$Py][$PF_6$]) for chemical modification of silica by means of the acid-catalyzed sol-gel processing[10]. The obtained RTIL-modified silica was employed as a solid phase extraction sorbent for removal of trace quantity of Fe(III) ions from aqueous samples. [$C_6$Py][$PF_6$] was also used as an extractant solvent in the preconcentration of trace quantity of zinc before its determination by flame atomic absorption spectrometry[11]. The combination of [$C_6$Py][$PF_6$]-based dispersive liquid-liquid micro-extraction (RTIL-based DLLME) with stopped-flow spectrofluorometry was applied to evaluate the concentration of aluminum Al(III) in different real samples at trace level[12]. Zeeb and Sadeghi proposed an efficient sample preparation method based on the application of [$C_6$Py][$PF_6$] as a microextraction solvent to preconcentrate and determine the trace quantity of Terazosin (a selective alpha-1 antagonist used for treatment of symptoms of an enlarged prostate) [13].

However, in all these studies, the water behavior of pyridinium-based RTILs was not investigated, while it is known that the presence of water molecules is important for the separation or extraction capacities of these solvents. [$C_6$Py][$PF_6$], an example of RTIL highly-cited in the above studies, was just qualified as hydrophobic RTIL. But it is known that the majority of RTILs is hygroscopic and can absorb water from ambient air despite their hydrophobic character[14-17]. Their hygroscopic capacity depends mainly on the nature of their ions (cation and anion), the relative humidity and the temperature. In addition, it is established that the physical and chemical properties of RTILs are very sensitive to water content[14-20]. Therefore, it is essential to evaluate the possible interactions between water and pyridinium-based RTILs in order to estimate the real potential of this family of RTILs.

Numerous studies have already examined the solubility of pyridinium-based RTILs in water. For example, Neves *et al.* determined the solubility of 1-methyl-3-propylimidazolium and 1-methyl-3-propylpyridinium cations combined with the [$PF_6$] anion in the temperature range from 288.15 to 318.15 K[21]. Freire *et al.* measured the solubility of imidazolium-, pyridinium-, pyrrolidinium-, and piperidinium-based RTILs in combination with different anions (bis-(trifluoromethylsulfonyl)imide, hexafluorophosphate, and tricyanomethane) in water between 288.15 and 318.15 K[22]. Yang *et al.* studied the solubility of 1-ethylpyridinium hexafluorophosphate in ethanol/water binary solvent mixture from 278.15 to 345.15 K[23]. Papaiconomou *et al.* studied the water solubility of RTILs containing 1-octylpyridinium, 1-octyl-2-methylpyridinium, or 1-octyl-4-methylpyridinium cations with various anions in two different experimental conditions, namely in equilibrium with the air and in the liquid water[24]. The solvatochromic solvent parameters of different RTILs based on imidazolium, hydroxyammonium, pyridinium and phosphonium cations at 298K using UV–Vis spectroscopy were studied[25]. However, to the best of our knowledge, no attempt has been made to quantify the possible interactions of water molecules and pyridinium-based RTILs in terms of both the water uptake and water behavior over the whole range of water activity.

The main objective of this work is to obtain a deeper understanding of the water sorption behavior of representative pyridinium-based RTIL, [$C_6$Py][$PF_6$], over the whole range of water activity. The choice of this IL is explained by the fact that this RTIL is among the most commonly used pyridinium-based RTILs in different fields of science. The measurements of water vapor sorption kinetics were carried out using the gravimetric method. The obtained water sorption isotherm was analyzed by using a two-mode sorption (Henry-clustering) in order to describe the water sorption behavior in [$C_6$Py][$PF_6$]. This model is based on the dual-model sorption idea, in which an ordinary dissolution (absorption)

described by Henry's law is combined with a clustering (aggregation) phenomenon. Water clustering involves multiple self-associated water molecules inside materials and it occurs mainly at high water activity. This model is the most appropriate as in this case the clustering phenomenon may be fitted separately from the Henry's linear part. The difference between the water sorption behavior of $[C_6Py][PF_6]$ and imidazolium-based RTILs, 1-hexyl-3-methylimidazolium hexafluorophosphate ($[C_6C_1im][PF_6]$, water-immiscible RTIL) and 1-butyl-3-methylimidazolium tetrafluoroborate ($[C_4C_1im][BF_4]$, water-miscible RTIL), was discussed. The application of the Zimm-Lundberg theory to water sorption isotherm results made it possible to determine the mean cluster size (MCS) of water molecules in $[C_6Py][PF_6]$, $[C_6C_1im][PF_6]$ and $[C_4C_1im][BF_4]$ as a function of the water concentration (or relative humidity). The infrared spectroscopy is extensively used for understanding the interactions between the water molecules and RTILs[14]. Therefore, the results of the water sorption were compared with the infrared spectroscopy results in order to discuss in details the molecular state of water molecules in RTILs.

## Experimental

1) Materials

The chemical structure of RTILs used in this work, i.e. $[C_6Py][PF_6]$, $[C_6C_1im][PF_6]$, and $[C_4C_1im][BF_4]$, is shown in Fig. 1. All RTILs were purchased from Acros Organics (> 99% purity) in liquid state and used as received. All water used was Milli-Q water (18.2 MΩ/cm at 25 °C, Millipore®). $N_2$ (99.99% purity, Air Products®) was used as received.

2) Sorption studies

The water vapor sorption kinetics measurements were carried out using a continuous gravimetric method. The electronic microbalance used was IGAsorp (Intelligent Gravimetric Analyser Sorption moisture) supplied by Hiden Isochema Limited (UK). At the beginning, studied RTIL was placed into a glass sample pan, and retained on one end of the electronic microbalance. The sample environment temperature was controlled by the thermoregulated water bath and fixed at 25.0 ± 0.2 °C. RTIL was dried by the dry flow of $N_2$ gas until a constant mass $m_0$ was obtained. Then, the water vapor pressure was increased gradually up to the saturated vapor pressure ($a$ = 0.95). At each activity level, the mass gain was continuously measured as a function of time until an equilibrium state was reached. The water vapor sorption isotherm was subsequently deduced by plotting the water content at equilibrium $M$ versus water activity:

$$M = \frac{m_{eq} - m_0}{m_0} = f(a) \quad \text{(Eq. 1)}$$

where $m_{eq}$ is the mass at the equilibrium state for a given water activity $a$.

3) Infrared spectroscopy

The infrared measurements were performed using the Fourier transform infrared (FTIR) Nicolet spectrometer (ThermoFischer, Avatar 360 Omnic Sampler) in an attenuated total reflectance (ATR) mode (Ge crystal) with a resolution of 8 $cm^{-1}$ with 200 scans per spectrum in the range of 4000 - 675 $cm^{-1}$.

The FTIR spectra of RTIL equilibrated with water vapors at a given vapor activity $a$ were obtained by means of a home-made apparatus developed for that purpose and explained in details in[26]. In short, dry RTIL was positioned inside a special hood placed over the sample compartment. The vapor generator was connected to the hood for a few hours, ensuring that RTIL was in the equilibrium state with the water vapor. Dry nitrogen and water-nitrogen flows were controlled with an electronic gas flowmeter (Agilent Technologies, 5067 model). The FTIR spectra were recorded for RTIL equilibrated with the water vapors (from $a = 0$ (i.e. dry RTIL) to $a = 0.95$) and liquid water (i.e. at $a = 1$).

**Theoretical background**

1) Two-mode sorption – Henry-clustering

The Flory-Huggins thermodynamic theory is used for correlating the penetrant sorption isotherms[27]. In this case, the sorption isotherm curve exhibits a quasi linear curve at low ($a \leq 0.2$) and intermediate ($0.2 < a \leq 0.7$) activity and then it is followed by a convex curvature for higher activity ($a > 0.7$). It is noted that this theory is useful for describing the water sorption behavior in a hydrophobic material[27]. Usually, the Flory-Huggins theory is applied for the organic solvent sorption in rubbery materials, for example, the chloroform sorption in silicone[28]. Perrin *et al.* showed that the water sorption isotherm in hydrophilic cellulose triacetate could also be well described by the Flory-Huggins theory, but only for the activity less than 0.7[29].

According to this theory, when a penetrant is added to the material solute, an enthalpy change can take place as the penetrant-penetrant and solute-solute interactions are replaced by the penetrant-solute interactions. It should be mentioned that the interactions between the penetrant and solute are assumed to be constant whatever the penetrant activity. However, the clustering phenomenon is not clearly explained as the deviation from the Flory-Huggins

thermodynamic theory is observed at high penetrant activity (≥ 0.7). Therefore, in the case of the RTIL water sorption isotherms with a curve shape similar to the Flory-Huggins sorption curve shape (i.e. the first linear part followed by the convex shape), it is more judicious to describe the isotherm by using an approach, which consists of two sorption modes: the Henry's dissolution and the clustering.

In the case of a binary system, the penetrant-penetrant and penetrant-material interactions are found to be dependent on the penetrant activity value. Thus, in our case it is assumed that two species of absorbed water molecules contribute to the water concentration in the material (RTIL): one of these species follows the Henry's law at low and intermediate water activity ($0 < a \leq 0.7$) (i.e. molecules are randomly sorbed in the medium with no specific interaction), and the second of the species at higher activity ($a > 0.7$) follows the water clustering (i.e. part of sorbed molecules from the Henry's sorption due to the predominant penetrant-penetrant interactions at high water concentration forms a cluster). Therefore, taking into account these two combined sorption modes, the water sorption isotherm may be expressed as follows:

$$C_{H_2O} = C_{(H_2O)_D} + nC_{(H_2O)_n} = k_D a + nK_a k_D^n a^n, \qquad \text{(Eq. 2)}$$

where $C_{H_2O}$ (g-water/g-RTIL) is the total water concentration, $C_{(H_2O)_D}$ and $nC_{(H_2O)_n}$ are the water concentration from the Henry's sorption and from the clustered species, respectively, $a$ is water activity, $k_D$ (g-water/g-RTIL) is the Henry's solubility coefficient representing the affinity of water molecules to the sample (RTIL), $n$ is the mean number of water molecules per cluster, and $K_a$ ((g-water/g-RTIL)$^{1-n}$) is the equilibrium constant for the clustering reaction.

The clustering formation corresponds to the next water equilibrium:

$$n\,H_2O \longleftrightarrow (H_2O)_n$$

which is characterized by an equilibrium constant $K_a$:

$$K_a = \frac{C_{(H_2O)_n}}{C_{H_2O}^n},$$

where $C_{H_2O}$ is the water concentration of free water molecules ($= k_D a$) and $C_{(H_2O)_n}$ is the concentration of the water clusters that can be determined as follows:

$$C_{(H_2O)_n} = nK_a C_{H_2O}^n = nK_a k_D^n a^n.$$

2) <u>Mean cluster size (MCS)</u>

The clustering theory of adsorbed molecules was proposed to explain some of the thermodynamic inconsistencies in sorption first by Zimm et Lundberg[30,31] and later by Starkweather[32]. Water is unique penetrant due to its polar nature, thus, it can create hydrogen bond with itself and can form clusters. This theory allows us to evaluate the degree of clustering in binary systems. At this mathematical approach, the clustering function is defined as:

$$\frac{G_S}{V_S} = -(1-\Phi_S)\left[\frac{\partial(a/\Phi_S)}{\partial a}\right]_{p,T} - 1, \qquad \text{(Eq. 3)}$$

where $G_S$ is the cluster integral, $V_S$, $\Phi_S$ and $a$ are the partial molar volume, the volume fraction and the activity of penetrant molecules (in our case, water molecules), respectively. The clustering function $\frac{G_S}{V_S}$ indicates whether clustering takes place or not and it can be easily determined from the experimental isothermal sorption[33,34]. A $\frac{G_S}{V_S}$ value equal to -1 (the case of the ideal solution, i.e. sorption isotherm following the Henry's law) indicates that penetrant molecules do not affect the distribution of other penetrant molecules. If $\frac{G_S}{V_S} > 0$, penetrant molecules tend to cluster provided the concentration is higher in their neighborhood as it would be expected on the basis of non-random mixing, whereas if a $\frac{G_S}{V_S}$ value is greater than -1, penetrant molecules prefer to remain isolated.

The expression $\frac{G_S\Phi_S}{V_S}$ represents the mean number of penetrant molecules in excess of the mean concentration. Thus, it measures the clustering tendency of penetrant molecules. The MCS value is hence an estimate of the mean number of molecules which exist in a cluster:

$$MCS = 1 + \left[\frac{\Phi_S G_S}{V_S}\right] \qquad \text{(Eq. 4)}$$

Following Starkweather[32], the equation for the mean size of a cluster can be written as:

$$MCS = (1-\Phi_S)\frac{a}{\Phi_S}\left(\frac{\partial\Phi_S}{\partial a}\right)_{p,T} \qquad \text{(Eq. 5)}$$

The volume fraction $\Phi_S$ is obtained from the relation:

$$\Phi_S = \left(1 + \frac{\rho_S}{M\rho_{IL}}\right)^{-1}, \quad \text{(Eq. 6)}$$

where $\rho_S$ and $\rho_{IL}$ are the densities of the penetrant (water) and sample (RTIL), respectively. The mass uptake $M$ at the equilibrium and at a given activity $a$ of sorbed species is defined according to Eq. 1. In the case of the Henry-clustering mode, the mass uptake can be expressed according to Eq. 2.

In the case of water transport studies, the Zimm and Lundberg theory has been often coupled with the approaches that allow obtaining a mathematical description of the water sorption isotherms. As a result, the MCS value can be expressed from the Henry-clustering parameters as follows:

$$MCS = \frac{\rho^2}{M^3(1+\frac{\rho}{M})^2}(k_D a + n^2 K_a k_D^n a^n), \quad \text{(Eq. 7)}$$

where $\rho = \frac{\rho_S}{\rho_{IL}}$. The densities of studied RTILs are 1.25 g/cm$^3$ for [$C_6$Py][$PF_6$], 1.31 g/cm$^3$ for [$C_6C_1$im][$PF_6$] and 1.21 g/cm$^3$ for [$C_4C_1$im][$BF_4$].

**Results and discussion**

1) Water sorption

The sorption kinetics of water vapor into a material depends on numerous factors, such as the chemical composition, the physical and chemical properties, etc. A continuous gravimetric analysis was performed in order to understand possible interactions of water molecules and [$C_6$Py][$PF_6$] over the whole range of water activity. Fig. 2 shows that the experimental data of the water vapor sorption kinetics of [$C_6$Py][$PF_6$] depend directly on the water activity $a$. As one can see, the water uptake increases with time to the achievement of the sorption equilibrium after certain period of time. Besides, the maximal amount of sorbed water increases when the water activity $a$ increases. Moreover, the sorption kinetics becomes longer starting from $a$ = 0.8. Before this value, the equilibrium state (i.e. gain mass plateau value) is reached rather rapidly (Fig. 2). The sorption kinetics provides a valuable insight into the mechanism involved in the transport of penetrate within a material. In order to get the details of the water sorption kinetics into RTIL, the water vapor sorption isotherm was obtained from the mass gain at the equilibrium state of the sorption kinetics according to Eq. 1

(Fig. 3). The water vapor sorption isotherms of imidazolium-based RTILs ([$C_6C_1$im][$PF_6$] and [$C_4C_1$im][$BF_4$]) (Fig. 1) obtained on the same conditions are added for comparison. The choice of [$C_6C_1$im][$PF_6$] is based on the fact that this RTIL is a well-known example of water-immiscible RTILs[1,2,14,15,19,35] and is known to have very weak interactions with water molecules even at high water activity, whereas [$C_4C_1$im][$BF_4$] is water-miscible RTIL[1,2,14,15,19,35] and is known for its strong water interaction capacity leading to the water clustering at high activity.

It can be seen from Fig. 3 that the water uptake by [$C_6$Py][$PF_6$] is quasi-linear and non-specific at low and intermediate water activity (up to $a < 0.8$), whereas at high water activity ($a > 0.8$), the water uptake increases exponentially.

The analysis of an adequate sorption isotherm model can give important information concerning the water organisation in the material. The water vapour isotherms have been already exploited and treated by classical thermodynamic models such as local-composition models, Group Contribution Methods[36], COSMO[37] and by other less classical models such as the modified RK EOS[38] and the Camper model[39]. As to the so-called local-composition models, one can find the non-random two-liquid model (NRTL)[40-42], the Wilson model[43], the UNIQAC model[44,45], and the group contribution model UNIFAC[46], but also GAB[47-49] and Park[50,51] models. Among all proposed in the literature models, it is admitted that GAB model is mostly used to describe the water sorption by food and food-stuffs. In the case of an exponential increase of the solvent concentration at high vapor pressure (i.e. in the case of the convex form of the isotherm) some other models can be also applied, e.g. Flory-Huggins, ENSIC, or aggregation models. For example, the Flory-Huggins model (usually used for vapor sorption in rubbery-elastomer materials) is not appropriate for polar penetrants such as water molecules (according to hypothesis of Flory-Huggins), so this model cannot be used for the ionic liquid/water system studied in the present work. The convex form of the isotherm is usually attributed to the typical water clustering phenomenon, and the strong increase of the water concentration at high water vapor pressure values is explained by the water/water interactions, which become predominant, compared to the water/substrate interactions. It is well known that such phenomenon occurs mainly in polar systems (i.e. in the case of hydrophilic materials) or in the system containing ionic groups, which are able to interact with water molecules, e.g. polyelectrolyte (Nafion®). In addition, as ionic liquids are liquid salts, so ion pairs can be easily solvated by water molecules, thus forming a hydration shell. Recently Zhu et al showed by means of a detailed NMR analysis that imidazolium cations with no or short alkyl chains can form a self-assembled clustering structure in water

283 solution[52]. The authors revealed the presence of the first hydration shell of the polar heads of
284 cations at the water concentration around 60 mol.%. Owing to the high mobility of ionic
285 liquids (i.e. low viscosity compared to polymer material), it is reasonable to imagine that
286 water molecules move and are bonded with each other by strong hydrogen bonds as in bulk
287 liquid water.
288 The presence of water clusters in ionic liquids is the well-known fact and it is
289 confirmed by both theoretical and experimental points of view. Being based on computation
290 studies of three ionic liquid systems containing [$BF_4$], [$PF_6$] and [$Tf_2N$] anions, Maiti et al.
291 revealed that the inclusion of small hydrogen-bonded water clusters was in better quantitative
292 agreement with the experimentally observed water sorption data[53]. Also, molecular dynamics
293 simulation (MDS) of mixtures of 1,3-dialkyl imidazolium ionic liquids and water performed
294 by Hanke and Lynden-Bell has shown that when the molar proportion of water molecules
295 reached 75%, a percolating network of water and small clusters was formed[54]. Singh and
296 Kumar examined the cation-anion-water interactions in aqueous mixtures of imidazolium
297 ionic liquids over the whole composition range using FTIR spectroscopy[55]. They showed the
298 existence of the hydration shell for [$BF_4$] anion and deduced the presence of water clusters
299 from the overall broad structure of the -OH band at 2800-3800 $cm^{-1}$. Moreover, by comparing
300 MDS results with the NMR data, Moreno et al. clearly showed that the ions were selectively
301 coordinated by individual water molecules at low water content, while the ionic network was
302 disrupted by the water clusters at high water content[56].
303 Taking into account the literature results mentioned above, in the present article the
304 dual-mode (Henry and clustering) was chosen. To evaluate how accurate the fitting was,
305 residual sum of squares (RSS) was used, i.e. the sum of squares of residuals (i.e. deviations
306 predicted from actual empirical values of data). RSS value allows measuring the discrepancy
307 between the experimental data and the estimation model. In each case, very small RSS values
308 were obtained indicating an accurate fit of the model to the experimental data. The fitted
309 model parameters ($k_D$, $K_a$ and n) (Eq. 2) are gathered in Table 1.
310 At low and intermediate water activity ($a \leq 0.8$), the water uptake by [$C_6Py$][$PF_6$]
311 increases linearly with the water activity value, revealing the typical Henry's sorption mode
312 (the first term in Eq. 2), for which interactions between water molecules are not predominant.
313 This sorption mode assumes a random dispersion of sorbed water molecules in RTIL. The
314 Henry's coefficient $k_D$ calculated from the curve slope illustrates the affinity of water
315 molecules and RTIL. The higher is the $k_D$ value, the higher is the water solubility in RTIL.
316 From the thermodynamical point of view, the [$C_6Py$][$PF_6$] water uptake is very low and quite

similar to that of $[C_6C_1im][PF_6]$ (Fig. 3), thus confirming their hydrophobic character. It can be noted that the $k_D$ values of $[C_6Py][PF_6]$ and $[C_6C_1im][PF_6]$ are rather close (Table 1) that explains the superposition of the water vapor sorption isotherms up to $a = 0.8$ (Fig. 3). It can be seen from Fig. 3 that the amount of water absorbed by $[C_4C_1im][BF_4]$ is largely higher than that absorbed by two $[PF_6]$-based RTILs at low and intermediate water activity. As a result, the $k_D$ value of $[C_4C_1im][BF_4]$ is almost ten times higher compared to that of $[C_6Py][PF_6]$ (Table 1). Thus, one can conclude that water molecules have very few interactions with $[C_6Py][PF_6]$ at low and intermediate activity, and that the behavior of $[C_6Py][PF_6]$ towards water is very similar to that of $[C_6C_1im][PF_6]$ (water-immiscible RTIL). This fact is in good agreement with the research of Papaiconomou *et al.*[24], who studied the water solubility of RTILs containing octylpyridinium-type cations, and found them nearly water immiscible. In addition, numerous studies indicate a weak water miscibility of $[PF_6]$-based RTILs because of the $[PF_6]$ anion presence[1,2,14,15,19,35]. Furthermore, it is interesting to note that $[C_6Py][PF_6]$ and $[C_6C_1im][PF_6]$ present almost the same interactions with water molecules up to $a = 0.8$ (Fig. 3), although the chemical structure of their cations is different (Fig. 1). It means that at low and intermediate water activity (i.e. at $a < 0.8$) the dialkylimidazolium cations and alkylpyridinium cations have approximately the same influence on the water sorption properties of RTILs (for the same anion). This result is consistent with the study of Neves *et al.*[21], who noted that the water solubility in 1-methyl-3-propylimidazolium and 1-methyl-3-propylpyridinium cations combined with the $[PF_6]$ anion is similar at 30°C.

At high water activity ($a > 0.8$), the strong increase in the $[C_6Py][PF_6]$ water uptake reveals the water clustering formation, which occurs also in $[C_4C_1im][BF_4]$ (Fig. 3). Consequently, the values of $K_a$ (the equilibrium constant for the clustering reaction) and $n$ (the mean number of water molecules per cluster) for these two RTILs are significantly higher in comparison with those for $[C_6C_1im][PF_6]$ (Table 1). Moreover, the values of $K_a$ and $n$ for $[C_6Py][PF_6]$ are surprisingly higher than those for $[C_4C_1im][BF_4]$, which is water-miscible RTIL. This means that water molecules are aggregated more easily in $[C_6Py][PF_6]$ than in $[C_4C_1im][BF_4]$. This result is very interesting, indicating, on the one hand, that the hydrophobicity of the cation increases from imidazolium- to pyridinium-based RTILs[21,22] and, on the other hand, that the role of anion in the water sorption and clustering in RTILs is a key one[14-16,18,19,35,44,55]. Indeed, it is well known that the $[BF_4]$ anion, compared to the $[PF_6]$ one, promotes the strong hydrogen bonds with and between water molecules[14,15,19,55,57], which explains both the strong water uptake and the formation of the water clusters in $[BF_4]$-based RTILs, compared to $[PF_6]$-based RTILs. These literature findings seem not to be valid for all

types of RTILs, but they are more suitable only for some classes of RTILs, such as imidazolium-based RTILs (the most extensively studied class in the literature). Consequently, it is not sufficient to take only the anion nature as an indicator of water miscibility in RTILs as it is shown in the present study that $[C_6Py][PF_6]$ which is $[PF_6]$-based RTIL has the highest values of $K_a$ and $n$ (Table 1) revealing an easier capacity for water molecules clustering compared to $[C_4C_1im][BF_4]$ (which is $[BF_4]$-based RTIL). This result could be due to the stronger dispersive interactions and, simultaneously, to the decreasing of cohesivity in pyridinium-based RTILs than in imidazolium-based RTILs[25]. The different kinds of water interactions with the π systems of aromatic cations (pyridinium and imidazolium cations) will be also responsible for this result[58].

The $[C_6Py]$ cation is of importance in the water clustering formation, even in combination with the $[PF_6]$ anion. This fact highlights the strong influence of the cation nature, in addition to that of anion, on the water sorption and clustering in pyridinium-based RTILs. Therefore, it is essential that the cation nature must be also taken into account in the study of interactions of water molecules and pyridinium-based RTILs. On the other hand, it is shown that $[C_6Py][PF_6]$ has a very low affinity towards water molecules at low and intermediate activity (the $k_D$ value (Table 1)). Thus, the behavior of pyridinium-based RTIL towards water molecules can be changed depending on water activity: $[C_6Py][PF_6]$ is water-immiscible RTIL at low and intermediate activity, thus limiting the water sorption, but at high activity ($a > 0.8$) the further sorption of water molecules on already sorbed monolayer moisture favours the water clustering formation as with the water activity increasing water/water interactions are largely stronger than water/RTIL ones. So, starting from a certain water concentration water molecules are self-associated to form clusters. Such behavior has been also observed in the case of the water sorption in low density polyethylene[59]. Indeed, the water cluster formation is revealed in this hydrophobic polymer with very low affinity towards polar molecules. The water clustering is explained by the hydrogen bonds between water molecules themselves confined in the matrix, thus leading to further reducing of the water mobility through the material. Therefore, for each given RTIL application, it is important first to determine the necessary water activity range. If the water presence in $[C_6Py][PF_6]$ is not desired at all, the operating conditions should be in the water activity range less than 0.8 in order to avoid the water sorption and clustering formation as much as possible. On the contrary, if the water presence is required, the RTIL can be applied at the water activity value close to 1. For other applications using pyridinium-based RTILs and where water is the reaction media (or is used in large quantity), the replacement of the $[PF_6]$

anion by others anions is recommended to further improve the water miscibility of RTIL. Popov *et al.*[60] used *N*-butyl-4-methyl-pyridinium tetrafluoroborate in aqueous solutions to measure the stability constants of crown-ether complexes with alkali-metal ions. This RTIL was qualified by Wang *et al.*[61] as water-soluble RTIL. It was used as a co-solvent with water by Riva *et al.*[62] to separate aromatic hydrocarbons from a naphtha of very low-aromatic-content (10 wt.%). Indeed, it is known that the different behavior of the $[BF_4]$ and $[PF_6]$ anions is attributed to the fact that the $[BF_4]$ van der Waals volume (48 $Å^3$) is smaller than the $[PF_6]$ one (68 $Å^3$), that gives more space for water molecules to be accommodated in $[BF_4]$-based RTILs[16,63]. Papaiconomou *et al.*[24] measured the water content of air-saturated and water-saturated pyridinium RTILs, 1-octyl-4-methylpyridinium tetrafluoroborate ($[4C_1C_8Py][BF_4]$), 1-octyl-2-methylpyridinium tetrafluoroborate ($[2C_1C_8Py][BF_4]$), 1-octyl-4-methylpyridinium trifluoromethyl sulfonate ($[4C_1C_8Py][TfO]$), and 1-octyl-4-methylpyridinium dicyanamide ($[4C_1C_8Py][N(CN)_2]$). At the equilibrium state with liquid water, the water content (in mass fraction) is 11.3, 13.6, 17.2 and 54.9% for $[4C_1C_8Py][BF_4]$, $[2C_1C_8Py][BF_4]$, $[4C_1C_8Py][TfO]$ and $[4C_1C_8Py][N(CN)_2]$, respectively. These values are much higher compared to 10.2% obtained for $[C_6Py][PF_6]$ at $a$ = 0.95. These pyridinium-based RTILs are, therefore, more water-miscible than $[C_6Py][PF_6]$ obviously due to the combination of the pyridinium-based cation with such anions as $[BF_4]$, $[TfO]$ and $[N(CN)_2]$.

Another question which arises is whether the water clustering mechanism in $[C_6Py][PF_6]$ is the same as in $[C_4C_1im][BF_4]$ (as no clustering is observed in $[C_6C_1im][PF_6]$ (see Fig. 3)). Fortunato *et al.*[63,64] studied the water uptake of imidazolium-based RTILs after their contact with aqueous solutions. The authors concluded that water molecules began to cluster on the molecular level only when the water content in RTIL exceeded a certain critical concentration. Scovazzo[65] indicated that the critical concentration for the water cluster formation is easier to reach for the water-miscible RTILs than for the water-immiscible RTILs. Dahi *et al.*[57] showed that the clustering process was linked to the affinity of water molecules and RTIL already at low and intermediate water activity: the higher the $k_D$ value, the higher the probability of the water clustering at high activity. From the obtained $k_D$ values (Table 1), it is clearly seen that the affinity or interactions of water molecules are very low in the case of $[C_6C_1im][PF_6]$ and rather high for $[C_4C_1im][BF_4]$ at low and intermediate water activity. This result allows us to explain why water molecules easily formed the clusters in $[C_4C_1im][BF_4]$ (high $K_a$ value, Table 1) in contrast with $[C_6C_1im][PF_6]$ (low $K_a$ value, Table 1) at high water activity. Indeed, it is known that the $[BF_4]$ anion promotes the strong hydrogen bonds with and between water molecules imidazolium-based RTILs compared to

the [$PF_6$] anion[14,15,19,44,55,57], which explains both the strong water uptake and the formation of the water clusters in [$C_4C_1$im][$BF_4$] compared to [$C_6C_1$im][$PF_6$]. However, in the case of [$C_6$Py][$PF_6$] (pyridinium-based RTIL), despite the low affinity with water at low and intermediate water activity (low $k_D$ value (Table 1), water molecules can easily form clusters in this RTIL at high activity, even more easily compared to [$C_4C_1$im][$BF_4$] (compare the $K_a$ values (Table 1)). Combining these results with the studies of Fortunato *et al.*[63,64], Scovazzo[65] and Dahi *et al.*[57], it can be pointed out that the water clustering mechanism in [$C_6$Py][$PF_6$] is different from that in [$C_4C_1$im][$BF_4$]. It seems that in the case of [$C_6$Py][$PF_6$], which is alkylpyridinium-based RTIL, the critical concentration for the water clustering formation is much lower in comparison to imidazolium-based RTILs. This fact may be explained by the RTIL cation structure. Wang *et al.*[58] studied hydrogen bonding interactions of 1-butylpyridinium tetrafluoroborate [$C_4$Py][$BF_4$] and water. They stated that water, when it forms the strong anion-HOH-anion complex, could also form H-bonds with aromatic C-H bond on the [$C_4$Py] cation. This result is different from the case of imidazolium-based RTILs, where the strong anion-cation interaction and steric hindrance from the alkyl chain length prevent water molecules to form H-bonding with aromatic C-H on the imidazolium cation, thus favouring interactions with the anion. This observation supports well the previously mentioned hypothesis about much stronger interactions of water molecules and the π systems of the pyridinium cations than of water molecules and the imidazolium cations.

In order to determine the activity from which the water clusters started to form in RTILs, the MCS value (Eq. 7) was calculated in addition to the $n$ parameter (Eq. 2), which represents roughly the number of water molecules per cluster. The calculated MCS values were plotted as a function of the water activity $a$ (Fig. 4). The MCS values are found to be close to unite at low water activity (below $a = 0.6$) for all three studied RTILs and clustering does not take place in this region. Then, the MCS values start to increase rapidly for [$C_6$Py][$PF_6$] and [$C_4C_1$im][$BF_4$], whereas for [$C_6C_1$im][$PF_6$] they stay still very low (~2 at $a = 0.95$). Such a result is expected as [$C_6C_1$im][$PF_6$] is water-immiscible RTIL over the whole range of water activity.

According to the Zimm-Lundberg theory, the MCS value greater than one is an indication of the cluster formation[30,31]. Thus, one can conclude that the water clustering starts from $a = 0.7$-$0.8$ for [$C_6$Py][$PF_6$] and [$C_4C_1$im][$BF_4$]. Starting from $a \approx 0.8$, further sorption of water molecules leads to the enhancement of water/water interactions and, thus, to the cluster formation. The formed hydrogen bonds between water molecules promote the rapid formation of a compact hydrogen bond network[57], which triggers the water clustering. As it can be seen

from Fig. 3, at $a$ = 0.8 the water sorption obtained for $[C_4C_1im][BF_4]$ (0.1075 g water/g RTIL) is higher than that for $[C_6Py][PF_6]$ (0.017 g water/g RTIL). At the same time, with the increase of water activity above 0.8, the MSC value increases much faster in the case of $[C_6Py][PF_6]$ compared to $[C_4C_1im][BF_4]$ (Fig. 4). It means that the water clustering process is more pronounced in $[C_6Py][PF_6]$ than in $[C_4C_1im][BF_4]$, thus allowing us to obtain rapidly larger water clusters in $[C_6Py][PF_6]$. This indicates again that the water clustering mechanism in $[C_6Py][PF_6]$ is different from that in $[C_4C_1im][BF_4]$. The obtained MCS plots based on the Zimm-Lundberg theory agree very well with the results of the Henry-clustering model. Indeed, the MCS value is equivalent to the $n$ parameter (the mean number of water molecules per cluster). However, the $n$ value depends strongly on the quality of the fit of the experimental data and, so, gives only an approximation of the cluster size (i.e. the average value), whereas the MCS value, derived from the statistical mechanics analysis, allows us to determine more precisely the mean size of cluster which varies with the environmental activity. From Fig. 4, one can easily see that the maximum value of MCS (at $a$ = 0.95) determined for $[C_6Py][PF_6]$, $[C_4C_1im][BF_4]$ and $[C_6C_1im][PF_6]$ is ~ 22, 12 and 2, respectively. These values are in good agreement with the calculated $n$ values (25, 19 and 3, respectively, Table 1), thus confirming the same tendency. The highest values of MCS and $n$ are found for $[C_6Py][PF_6]$ indicating a strong trend of water molecules to form clusters of large size (more than 20 water molecules per cluster) in this RTIL at high water activity.

2) Water molecular state

The measurement of the water clustering and interactions in a material is a key factor, however, the proposed structures and/or functions of water differ in many cases, and little consistency can be found among structures. Therefore, the water uptake should be also characterized by direct measurements using the infrared spectroscopy, where -OH bonds for different water populations have distinct bands and can be individually distinguished.

The IR bands corresponded to the water stretching vibration modes are widely used to study the molecular state of water dissolved in various solvents[66,67]. Two characteristic IR bands exist in the region of 3000-3800 $cm^{-1}$: the antisymmetric ($\nu_3$) and symmetric ($\nu_1$) stretching modes. Their intensity and position are strongly influenced both by the water environment and the water association *via* hydrogen bonding[14,19,55,57]. For example, in the case of the water vapor when water molecules are distant from each other, the $\nu_3$ and $\nu_1$ bands are situated at 3756 and 3657 $cm^{-1}$, respectively. In this case, water molecules are free (i.e.

they are not associated by hydrogen bonds). On the contrary, in the case of the liquid water, water molecules are linked by hydrogen bonds and these interactions trigger the overlapping of the $\nu_3$ and $\nu_1$ bands leading to a broad and intense band with a maximum at around 3300 $cm^{-1}$.

Fig. 5 shows the ATR-FTIR spectra of $[C_6Py][PF_6]$ in the region of the $\nu$(OH) stretching modes of water (3000-3800 $cm^{-1}$) obtained at different water activity. At the beginning, $[C_6Py][PF_6]$ was dried by the nitrogen flow ($a = 0$) in order to remove any residual water molecules. As a result, no characteristic IR bands of water were observed in the region 3000-3800 $cm^{-1}$ (Fig. 5). Then, $[C_6Py][PF_6]$ was progressively equilibrated at various water activity values (from 0 to 1).

No significant changes were noticed on the IR spectra up to $a = 0.82$. The absence of the water characteristic bands on the IR spectra of RTIL in the activity range from 0 to 0.8 may be explained by the very low water content in $[C_6Py][PF_6]$. This result confirms that $[C_6Py][PF_6]$ is water-immiscible RTIL at $0 < a < 0.8$. On the contrary, when $[C_6Py][PF_6]$ is equilibrated with water vapors at $a = 0.88$, a broad and intense band appears at 3360 $cm^{-1}$ (Fig. 5). The high intensity of this band and rapidity of its appearance proves a rapid and strong increase of the water content in $[C_6Py][PF_6]$ from $a = 0.82$ to $a = 0.88$. The sorption of a higher quantity of water molecules enhances significantly water/water interactions. As a result, sorbed water molecules start to interact together by hydrogen bonds. The shape and position of the band confirm the presence of intermolecular forces between water molecules, as the intense band results from the overlapping of the $\nu_3$ and $\nu_1$ bands[14,19,55,57]. Therefore, water molecules are well associated by hydrogen bonds at $a = 0.88$. This clustering starts probably even at $a = 0.82$ as the appearance of a large band around 3300 $cm^{-1}$ can be already observed on the spectrum at this water activity value (Fig. 5). This fact means that the activity value around 0.8 marks a crucial point in the behavior of $[C_6Py][PF_6]$ towards water. This observation conforms well to the MCS results (compare Fig. 4 and 5). The formed hydrogen bonds between water molecules promote the formation of a compact hydrogen bond network[57] and, subsequently, the formation of the water clusters. On the other hand, it does not seem necessary to reach a critical water content in $[C_6Py][PF_6]$ for the water association by hydrogen bonds and the formation of the water clustering since $[C_6Py][PF_6]$ reveals a low water content already at $a = 0.82$ (Fig. 5). This fact confirms the hypothesis proposed above that the water clustering mechanism in $[C_6Py][PF_6]$ is different from that in imidazolium-based RTILs. The increasing of water activity up to 1 promotes the increase of the intensity

and width of the water band (Fig. 5), i.e. further strengthening the hydrogen bond network. Consequently, water molecules sorbed in $[C_6Py][PF_6]$ form clusters or even droplets of the bulk liquid-like water at high water activity value. In addition, the shape of the band remains unchanged with the water activity increase, which would indicate that the molecular state of water in $[C_6Py][PF_6]$ is independent of the water concentration. According to numerous studies[14,17,55,57,68,69], the intense and broad band in the region around 3400 $cm^{-1}$ is attributed to water clusters. At high activity ($a$ > 0.8), water in $[C_6Py][PF_6]$ shows undoubtedly an easier capacity to be associated by hydrogen bonds until the water clustering formation.

The molecular state of water dissolved in different RTILs was studied by means of the infrared spectroscopy as a function of water activity[57]. Water molecules dissolved in $[C_4C_1im][PF_6]$ and $[C_6C_1im][PF_6]$ (water-immiscible RTILs) were found to be not self-associated by hydrogen bonds whatever the water content and, thus, they can be assigned as free water molecules. On the contrary, water molecules sorbed in $[C_4C_1im][BF_4]$, [$C_4$im][dibutylphosphate], [$C_4$im][bis(2-ethylhexyl)phosphate] and $[Et_3HN][CF_3SO_3]$ (water-miscible RTILs) were strongly associated with each other by the hydrogen bonds, and could be easily aggregated at high water activity. In the present study, although $[C_6Py][PF_6]$ is $[PF_6]$-based RTIL like $[C_4C_1im][PF_6]$ and $[C_6C_1im][PF_6]$, its behavior towards water at high activity is similar to that of above-mentioned water-miscible RTILs. The obtained IR results are in good agreement with the gravimetric analysis and the MCS results, and confirm the dual behavior of $[C_6Py][PF_6]$: water-immiscible RTIL from $a$ = 0 to $a$ = 0.8, and water-miscible RTIL at $a$ > 0.8.

## Conclusion

The water sorption properties of 1-hexylpyridinium hexafluorophosphate $[C_6Py][PF_6]$ were successfully investigated over the whole range of water activity. The experimental data of the water sorption isotherm were well fitted with the two-mode Henry-clustering model, and compared to those of imidazolium-based RTILs – $[C_4C_1im][BF_4]$ and $[C_6C_1im][PF_6]$. At low and intermediate water activity ($0 < a < 0.8$), the mass uptake was weak and, consequently, the affinity of water molecules and $[C_6Py][PF_6]$ was rather low. On the contrary, at $a$ > 0.8 the water uptake increases exponentially until the water clustering formation. The obtained results revealed that the water clustering mechanism in $[C_6Py][PF_6]$ is different from that in imidazolium-based RTILs. This proves the important influence of the cation structure, in addition to that of anion, on the water sorption of pyridinium-based RTILs.

The MCS values calculated according to the Zimm-Lundberg theory for $[C_6Py][PF_6]$, $[C_6C_1im][PF_6]$ and $[C_4C_1im][BF_4]$ were in good agreement with the results obtained by the Henry-clustering model. Both results indicate a strong trend of the water clustering in $[C_6Py][PF_6]$ starting from $a = 0.8$. This trend is much more pronounced than in $[C_4C_1im][BF_4]$ (water-miscible RTIL). It is concluded that the water sorption capacity of $[C_6Py][PF_6]$ varies so much with water activity that it can be considered as water-immiscible RTIL at the low and intermediate activity ($0 < a \leq 0.8$), and water-miscible RTIL at high water activity ($a > 0.8$).

The results of the sorption measurements were correlated with the molecular state of water dissolved in $[C_6Py][PF_6]$ studied by the infrared spectroscopy. At low and intermediate activity ($a \leq 0.8$), the water concentration in $[C_6Py][PF_6]$ was found to be low and, hence, $[C_6Py][PF_6]$ showed the behaviour of water-immiscible RTIL. On the contrary, at high activity ($a > 0.8$), the water concentration in $[C_6Py][PF_6]$ significantly increased. Water molecules were strongly associated with each other by the hydrogen bonds leading to the formation of a compact hydrogen bond network. Accordingly, water can easily form clusters. At high activity, $[C_6Py][PF_6]$ showed the behaviour of water-miscible RTIL. Although $[C_6Py][PF_6]$ belongs to $[PF_6]$-based RTILs, its strong water sorption and the water clustering at high activity must be taken into account for all applications when contact with water is necessary. The present study shows how the water sorption behavior of pyridinium-based RTILs can be modulated and controlled depending on the hydration conditions.

**Acknowledgements**

The authors acknowledge the financial support provided by the Réseaux Polymères Innovants (France). This work was partially supported by the ANR project Symposium (ANR-16-CE05-0005).

**References**

1 S. Keskin, D. Kayrak-Talay, U. Akman, O. Hortacsu, A review of ionic liquids towards supercritical fluid applications, J. Supercrit. Fluids 4 (2007) 150-180.

2 J. G. Huddleston, A. E. Visser, W. M. Reichert, H. D. Willauer, G. A. Broker, R. D. Rogers, Characterization and comparison of hydrophilic and hydrophobic room temperature ionic liquids incorporating the imidazolium cation, Green Chem. 3 (2001) 156-164.

3 J. F. Brennecke, E. J. Maginn, Ionic liquids: innovative fluids for chemical processing, AIChE J. 47 (2001) 2384-2389.

4 M. Freemantle, Eyes on ionic liquids. NATO workshop examines the industrial potential of green chemistry using room-temperature “designer solvents”, Chem. Eng. News 78 (2000) 37-50.

5 A.P. de los Ríos, F.J. Hernández Fernández, D. Gómez, M. Rubio, G. Víllora, Biocatalytic transesterification of sunflower and waste cooking oils in ionic liquid media, Process Biochem.46 (2011) 1475-1480.

6 J. M. Padró, R. B. P. Vidal, M. Reta, Partition coefficients of organic compounds between water and imidazolium-, pyridinium-, and phosphonium-based ionic liquids, Anal. Bioanal. Chem.406 (2014) 8021-8031.

7 C. Zhang, C. J. Dodge, S. V. Malhotra, A. J. Francis, Bioreduction and precipitation of uranium in ionic liquid aqueous solution by *Clostridium* sp., Biores. Technol. 136 (2013) 752-756.

8 D. Behar, P. Neta, C. Schultheisz, Reaction kinetics in ionic liuqids as studied by pulse radiolysis: redox reactions in the solvents methyltributylammonium bis(trifluoromethylsulfonyl)imide and *N*-butylpyridinium tertrafluoroborate, J. Phys. Chem. A 106 (2002) 3139-3147.

9 D. E. Siyutkin, A. S. Kucherenko, S. G. Zlotin, Hydroxy-α-amino acids modified by ionic liquid moieties: recoverable organocatalysts for asymmetric aldol reactions in the presence of water, Tetrahedron 65 (2009) 1366-1372.

10 H. Abdolmohammad-Zadeh, M. Galeh-Assadi, S. Shabkhizan, H. Mousazadeh, Sol-gel processed pyridinium ionic liquid – modified silica as a new sorbent for separation and quantification of iron in water samples, Arab. J. Chem. 9 (2016) S587-S594.

11 H. Abdolmohammad-Zadeh, G.H. Sadeghi, A novel microextraction technique based on 1-hexylpyridinium hexafluorophosphate ionic liquid for the preconcentration of zinc in water and milk samples, Anal. Chim. Acta 649 (2009) 211-217.

12 H. Abdolmohammad-Zadeh, G.H. Sadeghi, Combination of ionic liquid-based dispersive liquid-liquid micro-extraction with stopped-flow spectrofluorometry for the pre-concentration and determination of aluminum in natural waters, fruit juice and food samples, Talanta 81 (2010) 778-785.

13 M. Zeeb, M. Sadeghi, Sensitive determination of terazosin in pharmaceutical formulations and biological samples by ionic-liquid microextraction prior to spectrofluorimetry, Intern. J. Anal. Chem. 4 (2012) article ID 546282.

14 L. Cammarata, S. G. Kazarian, P. A. Salter, T. Welton, Molecular states of water in room temperature ionic liquids, Phys. Chem. Chem. Phys. 3 (2001) 5192-5200.

15 C. D. Tran, S. H. D. Lacerda, D. Oliveira, Absorption of water by room-tempearure ionic liquids: effect of anions on concentration and state of water, Appl. Spectrosc. 57 (2003) 152-157.

16 J. L. Anthony, E. J. Maginn, J. F. Brennecke, Solution thermodynamics of imidazolium-based ionic liquids and water, J. Phys. Chem. B 105 (2001) 10942-10949.

17 Y. Wang, H. Li, S. A. Han, A theoretical investigation of the interactions between water molecules and ionic liquids, J. Phys. Chem. B 110 (2006) 24646-24651.

18 K. R. Seddon, A. Stark, M. J. Torres, Influence of chloride, water, and organic solvents on the physical properties of ionic liquids, Pure Appl. Chem. 72 (2000) 2275-2287.

19 J. M. Andanson, F. Jutz, A. Baiker, Investigation of binary and ternary systems of ionic liquids with water and/or supercritical $CO_2$ by in situ attenuated total reflection infrared spectroscopy, J. Phys. Chem. B 114 (2010) 2111-2117.

20 J. S. Wilkes, M. J. Zaworotko, Air and water stable 1-ethyl-3-methylimidazolium based ionic liquids, J. Chem. Soc., Chem. Commun. 13 (1992) 965-967.

21 C. M. S. S. Neves, M. L. S. Batista, A. F. M. Claudio, L. M. N. B. F. Santos, I. M. Marrucho, M. G. Freire, J. A. P. Coutinho, Thermophysical properties and water saturation of $[PF_6]$-based ionic liquids, J. Chem. Eng. Data 55 (2010) 5065-5073.

22 M. G. Freire, C. M. S. S. Neves, P. J. Carvalho, R. L. Gardas, A. M. Fernandes, I. M. Marrucho, L. M. N. B. F. Santos, J. A. P. Coutinho, Mutual solubilities of water and hydrophobic ionic liquids, J. Phys. Chem. B 111 (2007) 13082-13089.

23 X.-Z. Yang, J. Wang, G.-S. Li, Z.-Z. Zhang, Solubilities of 1-ethylpyridinium hexafluorophosphate in ethanol+water from (278.15 to 345.15) K, J. Chem. Eng. Data 54 (2009) 75-77.

24 N. Papaiconomou, J. Salminen, J.-M. Lee, J. M. Prausnitz, Physicochemical properties of hydrophobic ionic liquids containing 1-octympyridinium, 1-octyl-2-methylpyridinium, or 1-octyl-4-methylpyridinium cations, J. Chem. Eng. Data 52 (2007) 833-840.

25 J. M. Padró, M. Reta, Solvatochromic parameters of imidazolium-, hydroxyammonium-, pyridinium- and phosphonium-based room temperature ionic liquids, J. Mol. Liq. 213 (2016) 107-114.

26 C. Chappey, K. Fatyeyeva, E. Rynkowska, W. Kujawski, L. Karpenko-Jereb, A.-M. Kelterer, S. Marais, Sulfonic membrane sorption and permeation properties:

complementary approaches to select a membrane for pervaporation, J. Phys. Chem. B 121 (2017) 8523-8538.

27 J. Barrie, B. Platt, The diffusion and clustering of water vapour in polymers, Polymer 4 (1963) 303-313.

28 E. Favre, P. Schaetzel, Q.T. Nguygen, R. Clément, J. Néel, Sorption, diffusion and vapor permeation of various penetrants through dense poly(dimethylsiloxane) membranes: a transport analysis, J. Membr. Sci. 92 (1994) 169-184.

29 L. Perrin, Q.T. Nguyen, D. Sacco, P. Lochon, Experimental studies and modelling of sorption and diffusion of water and alcohols in cellulose acetate, Polym. Int. 42 (1997) 9-16.

30 B.H. Zimm, J.L. Lundberg, Sorption of vapors by high polymers, J. Phys. Chem. 60 (1956) 425-428.

31 J.L. Lundberg, Molecular clustering and segregation in sorption systems, Pure Appl. Chem. 31 (1972) 261-282.

32 H.W. Strarkweather, Clustering of water in polymers, Polym. Lett. 1 (1963) 133-138.

33 P. Aranda, W.J. Chen, C.R. Martin, Water transport across polystyrenesulfonate/alumina composite membranes, J. Membr. Sci. 99 (1995) 185-195.

34 M.A. Del Nobile, G. Mensitiere, A. Sommazzi, Gas and water vapour transport in a polyketone terpolymer, Polymer 36 (1995) 4943-4950.

35 A. M. O'Mahony, D. S. Silvester, L. Aldous, C. Hardacre, R. G. Compton, Effect of water on the electrochemical window and potential limits of room-temperature ionic liquids, J. Chem. Eng. Data 53 (2008) 2884-2891.

36 M.D. Bermejo, T.M. Fieback, A. Martin, Solubility of gases in 1-alkym-3-methylimidazolium alkyl sulfate ionic liquids: experimental determination and modelling, J. Chem. Thermodyn. 58 (2013) 237-244.

37 X. Liu, W. Afzal, G. Yu, M. He, J.M. Prausnitz, High solubilities of small hybrocarbons in trihexyl tetradecylphosphonium bis(2,4,4-trimethylpentyl) phosphinate, J. Phys. Chem. B 113 (2013) 10534-10539.

38 M.B. Shiflett, D.R. Corbin, B.A. Elliott, A. Yokozeki, Sorption of trifluoromethane in zeolites and ionic liquid, J. Chem. Thermodyn. 64 (2013) 40-49.

39 D. Camper, J. Bara, C. Koval, R. Noble, Bulk-fluid solubility and membrane feasibility of Rmim-based room-termperature ionic liquids, Ind. Eng. Chem. Res. 45 (2006) 6279-6283.

688 40 A.-L. Revelli, F. Mutelet, J.-N. Jaubert, (Vapor+liquid) equilibria of binary mixtures
689 containing light alcohols and ionic liquids, J. Chem. Thermodyn. 42 (2010) 177-181.
690 41 H. Feng, Modeling of vapor sorption in glassy polymers using a new dual mode
691 sorption model based on multilayer sorption theory, Polymer 48 (2007) 2988-3002.
692 42 Y. Li, Q.T. Nguyen, K. Fatyeyeva, S. Marais, Water sorption behavior in different
693 aromatic ionomer composites analyzed with a "new dual-mode sorption" model,
694 Macromolecules 47 (2014) 6331-6342.
695 43 E. Zhao, M. Yu, R.E. Sauvé, M.K. Khoshkbarchi, Extension of the Wilson model to
696 electrolyte solutions, Fluid Phase Equilib. 173 (2000) 161-175.
697 44 J.A. Lazzus, J. Martin, Activity coefficient models to describe isothermal vapor-liquid
698 equilibrium of binary systems containing ionic liquids, J. Eng; Thermophys. 19 (2010)
699 170-183.
700 45 M. Kahrizi, N. Kasiri, T. Mohammadi, S. Zhao, Introducing sorption coefficient
701 throught extended UNIQAC and Flory-Huggins models for improved flux prediction
702 in forward osmosis, Chem. Eng. Sci. 198 (2019) 33-42.
703 46 H. Kuramochi, K. Maeda, S. Kato, M. Osako, K. Nakamura, S.-i. Sakai, Application
704 of UNIFAC models for prediction of vapor-liquid and liquid-liquid equilibria relevant
705 to separation and purification processes of crude biodiesel fuel, Fuel 88 (2009) 1472-
706 1477.
707 47 E.O. Timmermann, J. Chirife, H.A. Iglesias, Water sorption isotherms of foods and
708 foodstuffs: BET or GAB parameters? J. Food ENg. 48 (2001) 19-31.
709 48 D.J. Sampson, Y.K. Chang, H.P. Vasantha Rupasinghe, Q. UZ Zaman, A dual-view
710 computer-vision system for volume and image yexture analysis in multiple apple slices
711 drying, J. Food ENg. 127 (2014) 49-57.
712 49 V. Klika, J. Kubant, M. Pavelka, J.B. Benziger, Non-equilibrium thermodynamic
713 model of water sorption in Nafion membranes, J. Membr. Sci. 540 (2017) 35-49.
714 50 C. Mericer, M. Minelli, M.G. Baschetti, T. Lindstrom, Water sorption in
715 microfibrillated cellulose (MFC): the effect of temperature and pretreatment,
716 Carbohyd. Polym. 174 (2017) 1201-1212.
717 51 K. Fatyeyeva, S. Rogalsky, O. Tarasyuk, C. Chappey, S. Marais, Vapour sorption and
718 permeation behaviour of supported ionic liquid membranes: application for organic
719 solvent/water separation, React. Function. Polym. 130 (2018) 16-28.

720 52 H. Zhu, R. Vijayaraghavan, D. R. MacFarlane, M. Forsyth, Self-assembled structure
721 and dynamics of imidazolium-based protic salts in water solution, Phys. Chem. Chem.
722 Phys. 21 (2019) 2691-2696.
723 53 A. Maiti, A. Kumar, R. D. Rogers, Water-clustering in hygroscopic ionic liquids -an
724 implicit solvent analysis, Phys. Chem. Chem. Phys. 14 (2012) 5139-5146.
725 54 C. G. Hanke, R. M. Lynden-Bell, A simulation study of water - dialkylimidazolium
726 ionic liquid mixtures, J. Phys. Chem. B 107 (2003) 10873-10878.
727 55 T. Singh, A. Kumar, Cation-anion-water interactions in aqueous mixtures of
728 imidazolium based ionic liquids, Vib. Spectrosc. 55 (2011) 119-125.
729 56 M. Moreno, F. Castiglione, A. Mele, C. Pasqui, G. Raos, Interaction of water with the
730 model ionic liquid [bmim][BF4]: molecular dynamics simulations and comparison
731 with NMR data, J. Phys. Chem. B 112 (2008) 7826-7836.
732 57 A. Dahi, K. Fatyeyeva, C. Chappey, D. Langevin, S. P. Rogalsky, O. P. Tarasyuk, S.
733 Marais, Water sorption properties of room-temperature ionic liquids ver the whole
734 range of water activity and molecular states of water in these media, RSC Adv. 5
735 (2015) 76927-76938.
736 58 N.-N. Wang, Q.-G. Zhang, F.-G. Wu, Q.-Z. Li, Z.-W. Yu, Hydrogen bonding
737 interactions between a representative pyridinium-based ionic liquid [BuPy][BF4] and
738 water/dimethyl sulfoxide, J. Phys. Chem. B 114 (2010) 8689-8700.
739 59 S. Marais, Q. T. Nguyen, D. Langevin, M. Métayer, Transport of water and gases
740 through EVA copolymer films, $EVA_{70}$/PVC, and $EVA_{70}$/PVC/gluten blends,
741 Macromol. Symp. 175 (2001) 329-347.
742 60 K. Popov, H. Rönkkömäki, M. Hannu-Kuure, T. Kuokkanen, M. Lajunen, A. Vendilo,
743 P. Oksman, L. H. J. Lajunen, Stability of crown-ether complexes with alkali-metal
744 ions in ionic liquid-water mixed solvents, J. Incl. Phenom. Macrocycl. Chem. 59
745 (2007) 377-381.
746 61 L. Wang, H. Sun, G. Zhang, S. Sun, X. Fu, Heavy metal pollution of the world largest
747 antimony mine-affected agricultural soils in Hunan province (China), J. Soils
748 Sediments 13 (2013) 450-456.
749 62 J. de Riva, V.R. Ferro, D. Moreno, I. Diaz, J. Palomar, Aspen Plus supported
750 conceptual design of the aromatic-aliphatic separation from low aromatic content
751 naphtha using 4-methl-N-butylpyridinium tetrafluoroborate ionic liquid, Fuel Proces.
752 Technol. 146 (2016) 29-38.

753 63 R. Fortunato, C. A. M. Afonso, M. A. M. Reis, J. G. Crespo, Supported liquid
754 membranes using ionic liquids: study of stability and transport mechanisms, J. Membr.
755 Sci. 242 (2004) 197-209.
756 64 R. Fortunato, M. J. Gonzalez-Munoz, M. Kubasiewicz, S. Luque, J. R. Alvarez, C. A.
757 M. Afonso, I. M. Coelhoso, J. G. Crespo, Liquid membranes using ionic liquids: the
758 influence of water on solute transport, J. Membr. Sci. 249 (2005) 153-162.
759 65 P. Scovazzo, Testing and evaluation of room temperature ionic liquid (RTIL)
760 membranes for gas dehumidification, J. Membr. Sci. 355 (2010) 7-17.
761 66 E. Zoidis, J. Yarwood, T. Tassaing, Y. Danten, M. Besnard, Vibrational spectroscopic
762 studies on the state of aggregation of water in carbon tetrachloride, in dioxane and in
763 the mixed solvents, J. Mol. Liq. 64 (1995) 197-210.
764 67 H. Kusanagi, S. Yukawa, Fourier transform infra-red spectroscopic studies of water
765 molecules sorbed in solid polymers, Polymer 35 (1994) 5637-5640.
766 68 Y. Danten, M. I. Cabaço, M. Besnard, Interaction of water diluted in 1-butyl-3-methyl
767 imidazolium ionic liquids by vibrational spectroscopy modeling, J. Mol. Liq. 153
768 (2010) 57-66.
769 69 P. A. Bergstrom, J. Lindgren, O. Kristiansson, An IR study oft he hydration of $ClO_4^-$,
770 $NO_3^-$, $I^-$, $Br^-$, $Cl^-$, and $SO_4^{2-}$ anions in aqueous solution, J. Phys. Chem. 95 (1991)
771 8575-8580.

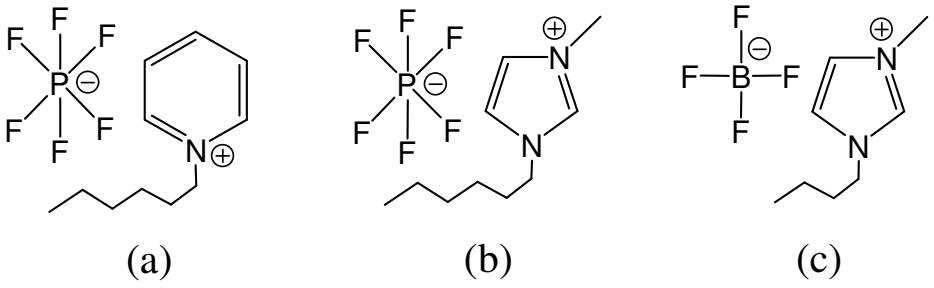


**Fig. 1**. Chemical structure of (a) $[C_6Py][PF_6]$, (b) $[C_6C_1im][PF_6]$, and (c) $[C_4C_1im][BF_4]$.

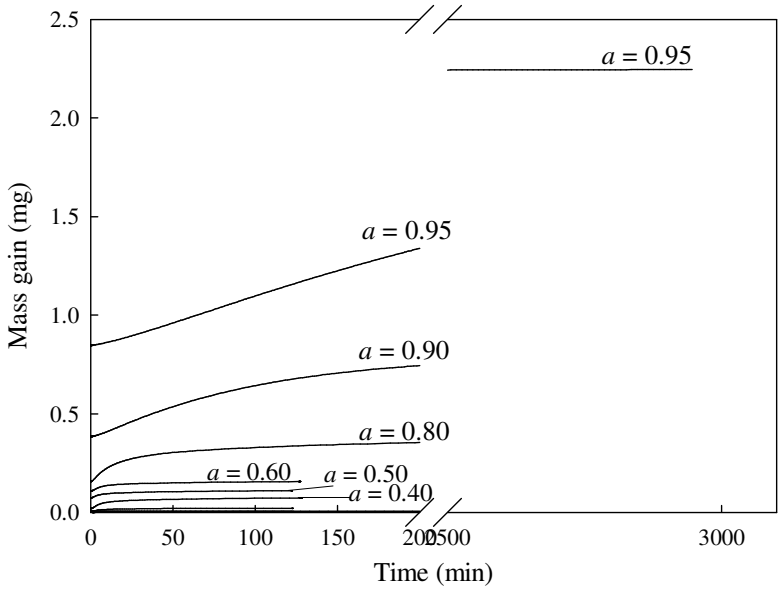


**Fig. 2.** Water vapor sorption kinetics of $[C_6Py][PF_6]$ at different water activity values.

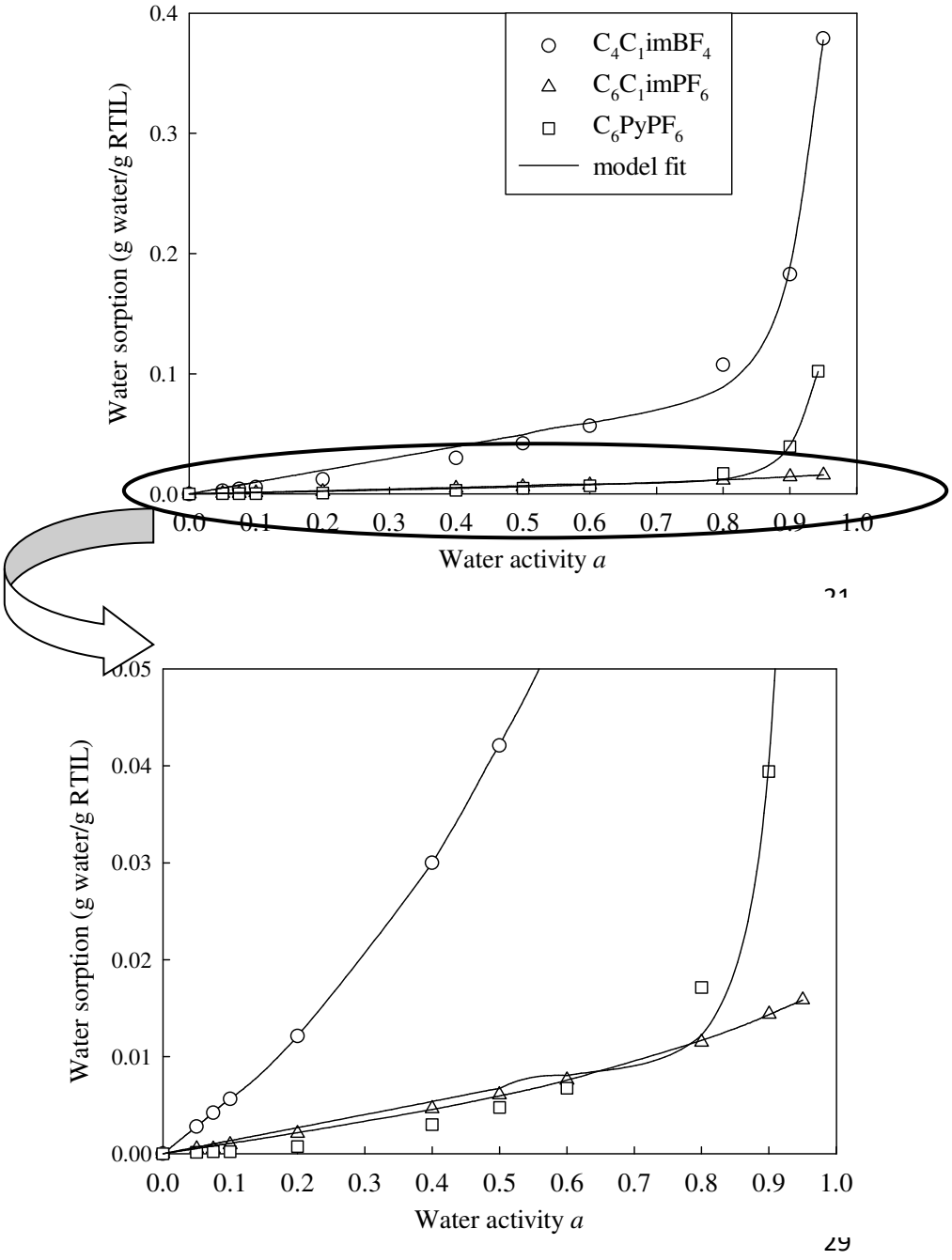


**Fig. 3.** Water vapor sorption isotherms of different RTILs. Solid lines are the fit according to the Henry-clustering model (Eq. 2).

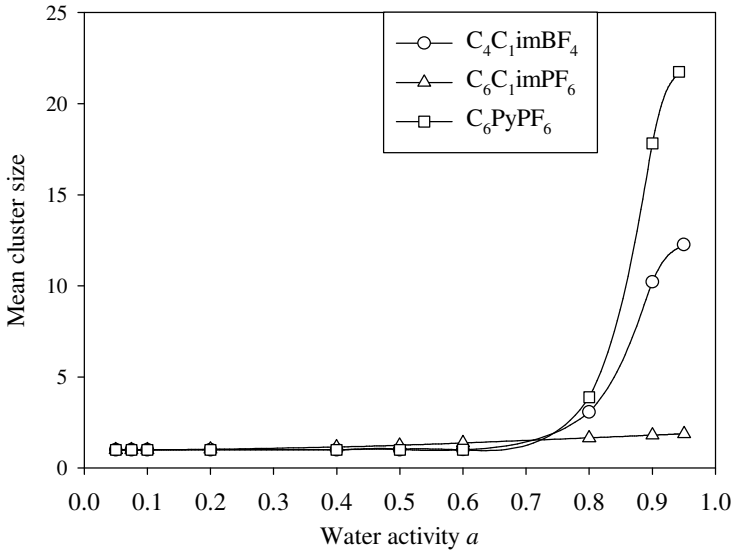


**Fig. 4.** Mean cluster size of $[C_6Py][PF_6]$, $[C_6C_1im][PF_6]$ and $[C_4C_1im][BF_4]$ as a function of water activity.

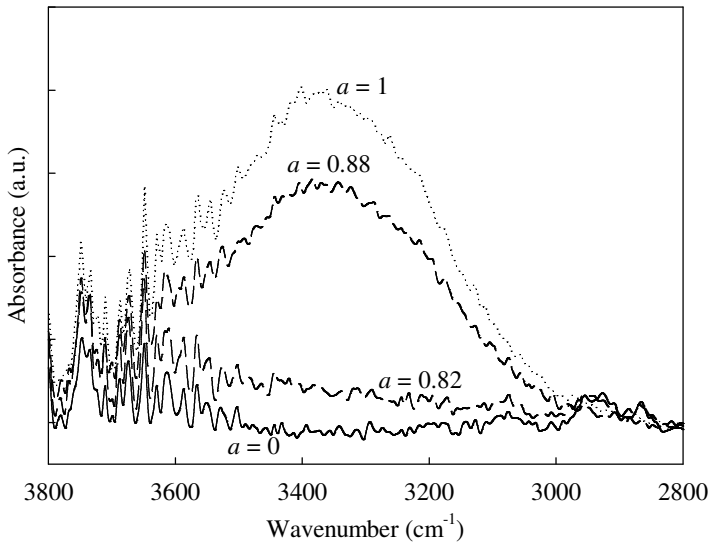


**Fig. 5.** ATR-IR spectra of $[C_6Py][PF_6]$ as a function of water activity $a$.

**Table 1.** Parameters of the Henry-clustering model (Eq. 2).

| RTIL | Parameter | | | Ref. |
|---|---|---|---|---|
| | $k_D$ (g water/g RTIL) | $K_a$ ((g water/g RTIL)$^{1-n}$) | $n$ | |
| $[C_6Py][PF_6]$ | $1.3 \cdot 10^{-2}$ | $1.4 \cdot 10^{45}$ | 25.1 | This work |
| $[C_6C_1im][PF_6]$ | $1.1 \cdot 10^{-2}$ | $1.2 \cdot 10^{4}$ | 3.5 | [36] |
| $[C_4C_1im][BF_4]$ | $9.8 \cdot 10^{-2}$ | $1.2 \cdot 10^{18}$ | 19.3 | [36] |